01 Aug 2003

Anticipating Vehicle-Level EMI using a Multi-Step Approach

Geping Liu

David Pommerenke
Missouri University of Science and Technology, davidjp@mst.edu

James L. Drewniak
Missouri University of Science and Technology, drewniak@mst.edu

Richard W. Kautz

et. al. For a complete list of authors, see https://scholarsmine.mst.edu/ele_comeng_facwork/1453

Recommended Citation

Anticipating Vehicle-Level EMI Using A Multi-Step Approach

Geping Liu, David J. Pommerenke, James L. Drewniak,

Richard W. Kautz* and Chingchi Chen*

Electromagnetic Compatibility Laboratory
Department of Electrical and Computer Engineering
University of Missouri-Rolla, Rolla, MO, 65401
Email address: geping@umr.edu

* Ford Motor Company
Dearborn, MI, 48121-2053
Email address: cchen4@ford.com, rkautz1@ford.com, and
kfrazie1@ford.com

Abstract

A multi-step procedure for anticipating vehicle-level EMI is proposed in this paper. This approach uses multi-conductor transmission line (MTL) modeling to calculate current distributions along the cable bundle. A common-mode circuit is extracted from the MTL modeling, and is employed in full-vehicle full-wave modeling to determine radiation and interference. In this paper, mode-dispersion and mode-conversion phenomena are investigated, and the ambiguous definitions of the common-mode voltage and common-mode impedance are discussed.

Keywords

Multi-conductor transmission line (MTL), finite-difference time-domain (FDTD), mode-dispersion, mode-conversion, common-mode current, common-mode voltage, common-mode impedance.

INTRODUCTION

Electromagnetic interferences (EMI) caused by high-speed digital control electronics, as well as power electronics, may prevent commercial vehicles from satisfying stringent EMC criteria. The cable bundles connecting controllers and loads, with small cross-section dimensions as compared to the larger car body, limits the application of 3D full-wave analysis in EMC design. Indeed, the mesh size required to describe wires inside a cable bundle is too small, and leads to an enormous demand for computer memory. Therefore, an appropriate multi-wire model for 3D full-wave analysis can significantly shorten the full vehicle-level modeling time, whether dealing with electromagnetic interference or susceptibility problems. Related work for modeling cable bundles is reviewed herein. A method of combining MTL and 3D BEM modeling is proposed to solve the automotive EMC problems [1], [2]. A methodology is presented to apply Agrawal's model in a numerical simulation of an electromagnetic susceptibility problem up to 500 MHz [3]. Based on the concepts of EM topology, this methodology consists of calculating the incident fields with a 3D full wave analysis (FDTD) and the coupling on the cables with MTL modeling.

However, the coupling models, proposed in [1], [2], [3], between the external environment and the harness are constructed in a fashion that is not seamless, since the 3D full-wave analysis and MTL modeling have to be implemented sequentally. Thus, a multi-wire formalism for FDTD is proposed based on the initial thin-wire-formalism [5], and

it can deal with multiple parallel and very close wires [4]. Multiple, closely coupled wires could be modeled by solving simultaneous, coupled equations for the wire bundle concurrently with the FDTD time stepping. However, implementation of a set of terminations for the cable bundle embedded in an FDTD cell was not addressed. A fully integrated model of coupling for the transmission-line matrix (TLM) method has been proposed in [6]. A fictitious cylinder sheath around a cable bundle is constructed as the reference conductor to account for the common-mode currents, while the actual N-conductor cable bundle can be specified inside the virtual sheath by MTL modeling. Thus, this method indirectly indicates that common-mode radiation is dominant, and mode-conversion is considered by the voltage source between different segments of the reference line, i.e., the virtual sheath.

In this paper, as a part of the multi-step procedure for anticipating vehicle-level EMI, an easily accessible single-wire common-mode model is extracted from MTL modeling of a cable bundle, and incorporated into FDTD formulation. Essentially, this model extracts a common-mode circuit through which the same common-mode current on the cable bundle flows, and exposes the inherent differential-to-common-mode conversion mechanism. Herein the common-mode circuit is defined as having a current that travels down the cable bundle, but unintentionally returns on the vehicle chassis and ultimately illuminates the whole vehicle. Therefore, this single-wire model might be suitable for a cable bundle consisted of closely spaced wires since the common-mode radiation is dominant. However, the problems of concern include in which case the single-wire model is effective, how to determine the necessary parameters of a single-wire model. When an extracted single-wire common-mode model is applied for predicting EMI, two inherent physical phenomena, i.e., mode-dispersion and mode-conversion, are discovered. Two important yet ambiguous concepts, e.g., common-mode voltage, common-mode impedance, are discussed. Actually, the phenomena and concepts directly influence the construction of an extracted common-mode circuit.

INFLUENCES OF MODE-DISPERSON AND MODE-CONVERSION

In the case of harnesses over the chassis, which is the most common configuration in automotives, the TEM mode or quasi-TEM mode becomes preponderant as compared to the antenna-mode [7], [3]. Therefore, a MTL modeling

generally provides good estimates for currents and voltages of a multi-wire cable bundle above ground plane.

A general multi-conductor line consists of a number of parallel conductors of arbitrary cross section, but uniform in the third dimension. For a N + 1 conductor line, a similarity transformation can decouple them into N uncoupled, two-conductor lines (or N uncoupled modes), with respect to the (N + 1)th reference conductor, i.e., the ground plane [8]. Each uncoupled, two-conductor line has its own characteristic impedance, velocities of propagation, mode voltages, and mode currents. At both ends of the multi-conductor line, or discontinuity locations of the line, mode conversion exists to interact the N uncoupled modes. When the medium surrounding the conductors is homogenous, e.g., bare wires in the air, all uncoupled modes have the same velocity. When the medium is inhomogeneous, the velocity of each uncoupled mode may be different.

In an inhomogeneous environment, the existence of mode-dispersion phenomenon, due to the different velocities of the N uncoupled modes, may influence the extraction of a single-wire common-mode circuit. A time-domain MTL analysis can clearly illustrate the mode-dispersion phenomenon of a common-mode current waveform in Case 1 shown in Figure 1. An 86-cm long 6-wire ribbon cable is placed very close to the ground plane, and terminated with loads, as shown in Table 1. A 2D field solver can extract per-unit-length capacitance and inductance matrices C and L based on the cross section shown in Figure 1(b). Therefore, a lossless time-domain MTL (N = 6) model is constructed when a common-mode voltage source having a narrow Gaussian-pulse excites Wire 3, as shown in Figure 2.

Table 1. Source and load terminations in Case 1 and Case 3

| Terminations in the source box	Terminations in the load box
Wire1-to-GND: open (≈10 MΩ)	Wire1-to-GND: 50Ω SMT resistor
Wire2-to-GND: open (≈10 MΩ)	Wire2-to-GND: 50Ω SMT resistor
Wire3-to-GND: semi-rigid coaxial feeding cable	Wire3-to-GND: short
Wire4-to-GND: short	Wire4-to-GND: short
Wire5-to-GND: open (≈10 MΩ)	Wire5-to-GND: 50Ω SMT resistor
Wire6-to-GND: open (≈10 MΩ)	Wire6-to-GND: 50Ω SMT resistor

Herein the common-mode current of a cable bundle is defined as the summation of all currents on each wire inside the bundle, i.e.,

$$I_{cm}(z) = \sum_{i=1}^{6} I_i(z),\qquad (1)$$

where the propagation diction is along z-axis, and it unintentionally returns back on the vehicle chassis.

(a)

(b)
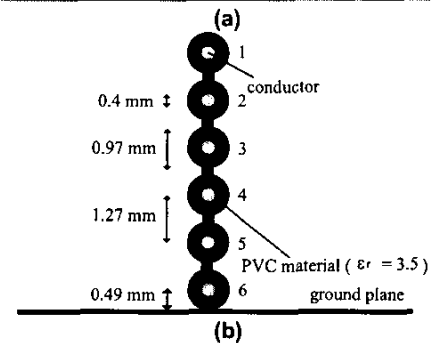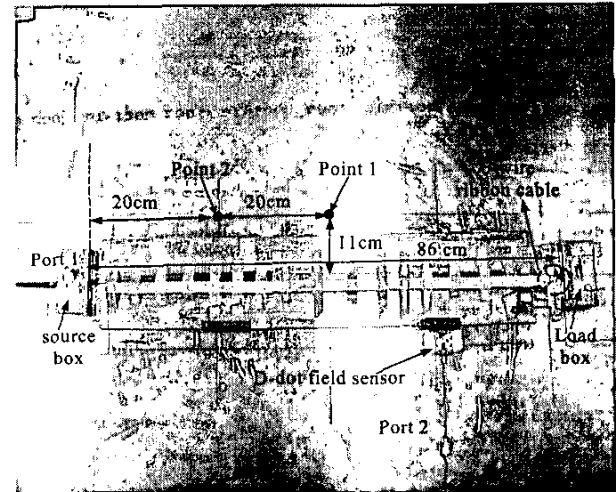
Figure 1. Measurement setup of a uniform 6-wire ribbon cable in Case 1 and Case 2: (a) the ribbon cable connecting to the source and load box above the ground plane; (b) 2D cross section of the ribbon cable.
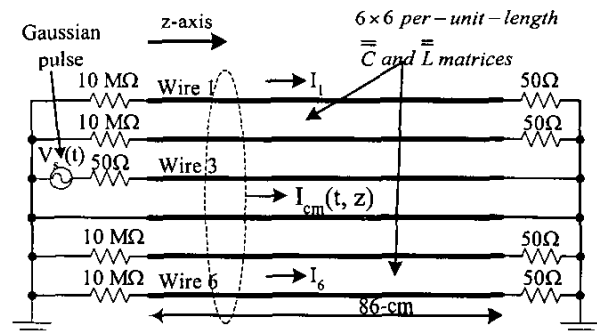
Figure 2. Time-domain MTL model for the ribbon cable in Case 1.

The common-mode current $I_{cm}(z, t)$ of the 6-wire ribbon cable calculated by the MTL modeling is shown in Figure 3. At time = 0, a forward-traveling common-mode current wave having Gaussian shape is initially excited by the voltage source feeding Wire 3, and propagated down the line. Because the common-mode current wave consists of six mode-currents that have six different velocities, its waveform is distorted, and it can derive six basic shapes corresponding to the six uncoupled modes. The phenomenon is

420

commonly called mode-dispersion, and it only occurs in inhomogeneous environment. When the common-mode current wave reaches the source, load, or other discontinuity positions, the mode-conversion exacerbate or alleviate the mode-dispersion since the six uncoupled modes interact with each other. In Case 1, the termination configuration shown in Table 1 seems to deteriorate the inherent mode-dispersion. Therefore, a single-wire common-mode circuit model cannot extract the common-mode current of the ribbon cable correctly, thereby not predicting well the electric fields at Point 1 and Point 2 in Case 1, as shown in Figure 4. An alternative approach is to construct six single-wire common-mode circuit models that correspond to six uncoupled-modes, respectively. Thus the total common-mode current and electric field are obtained using superposition theory. However, this approach is time-consuming.
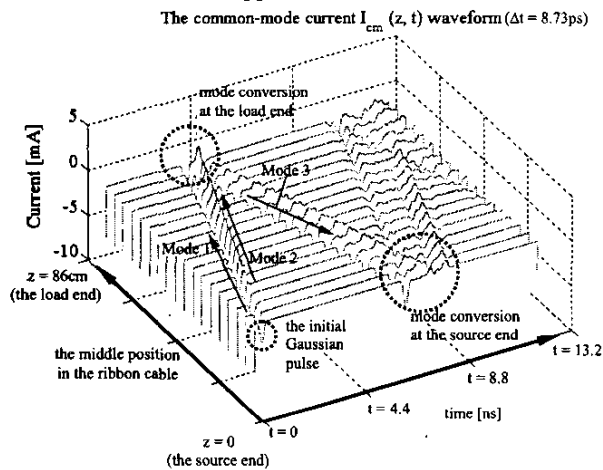
Figure 3. Propagation of the common-mode current waveform along the ribbon cable excited by a Gaussian pulse.
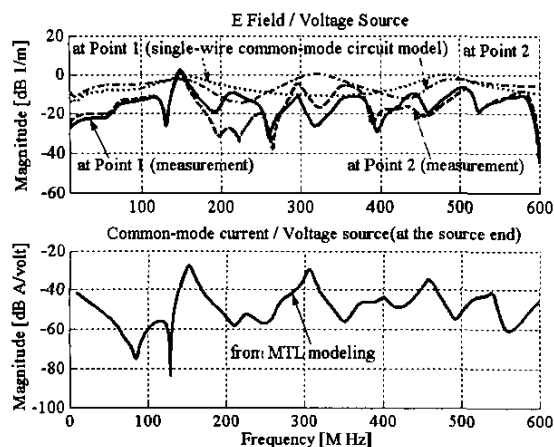
Figure 4. Electric fields at Point 1 and Point2, and calculated common-mode current at the source end in Case 1.

Table 2. Source and load terminations in Case 2.

Terminations in the source box	Terminations in the load box
Wire1-to-GND: 50Ω SMT resistor	Wire1-to-GND: 50Ω SMT resistor
Wire2-to-GND: 50Ω SMT resistor	Wire2-to-GND: 50Ω SMT resistor
Wire3-to-GND: semi-rigid coaxial feeding cable	Wire3-to-GND: 50Ω SMT resistor
Wire4-to-GND: 50Ω SMT resistor	Wire4-to-GND: 50Ω SMT resistor
Wire5-to-GND: 50Ω SMT resistor	Wire5-to-GND: 50Ω SMT resistor
Wire6-to-GND: 50Ω SMT resistor	Wire6-to-GND: 50Ω SMT resistor

When the terminations of the same 86-cm long ribbon cable are all changed to 50Ω SMT resistors (Case 2), as shown in Table 2, it significantly alleviates the mode-dispersion. When the equivalent height (h^{equ}) of the single-wire common-mode circuit is approximately selected as 4.25-mm, the equivalent radius (a^{equ}) is estimated as 1.4-mm using an empirical equation [5], and the common-mode source and load impedances of the single-wire are considered as the parallel configurations of the six 50Ω resistors, approximately 8.33Ω, then the single-wire can be implemented by the sub-cellular thin wire algorithm in FDTD code [9].
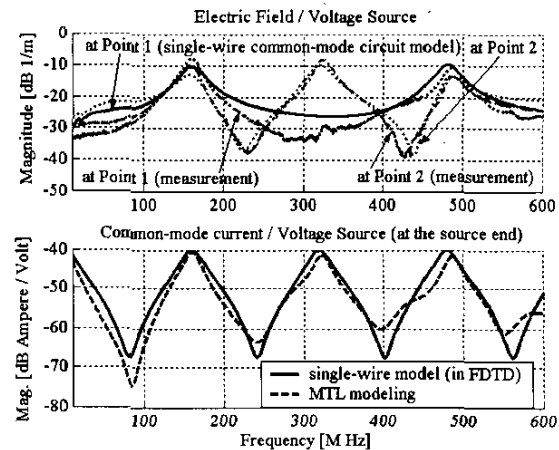
Figure 5. Electric fields at Point 1 and Point2, and common-mode currents at the source end in Case 2.

The calculated common-mode current at the source end from FDTD modeling is compared with that from MTL modeling, and the calculated electric fields at Point 1 and Point 2 compared with the measured electric fields in Figure 5. The common-mode currents and the electric fields are absolutely different from those results in Figure 4. The reason may be explained that more resistive loads in Case 2 quickly suppress other weak modes, and only primary mode of the common-mode current continues to travel at a certain velocity. Thus the mode-dispersion is weak, and the single-wire common-mode circuit model works better than that in Case 1. In Case 2, the peaks of the common-mode currents and the electric fields associate with the half-wavelength resonance of the ribbon cable. In addition, it is noticed that the single-wire model becomes more effective when the spacing between the ribbon cable and the ground plane is increased.

421

DEFINITION OF COMMON-MODE IMPEDANCE AND COMMON-MODE VOLTAGE

For a multi-conductor transmission line above a ground plane, there is no unique common-mode impedance definition, as well as the common-mode voltage definition. Still, there is a unique common-mode current definition, i.e., (1). Although not uniquely defined, the common-mode impedance is used in a multitude of papers, and EMC standards like CISP22 and IEC 61000-4-6. The common-mode loop impedance concept is proposed in Dual-Current-Probe measurement instead of the ambiguous common-mode impedance [10]. Thus care should be exercised for using the two terms.

EXTRACTION OF A SINGLE-WIRE COMMON-MODE CIRCUIT IN THE HOMOGENOUS CASE

Since there is no mode-dispersion phenomenon in homogeneous case, a single-wire common-mode circuit is believed to exist, and it can effectively represent a cable bundle in 3D full-wave analysis for predicting EMI. Reasonable approaches are conducted to determine parameters of a single-wire common-mode circuit.

A 90-cm long uniform six-wire bundle connecting the source and load box is placed close to the ground plane, as shown in Figure 6(a), and its 2D cross section is shown in Figure 6(b). Its terminations are listed in Table 1. First, a 2D field solver extracts per-unit-length capacitance and inductance matrices C and L of the homogenous wire bundle. Second, a lossless MTL model is constructed in time-domain or frequency-domain, and six-current and six-voltage distributions along the bundle are calculated.

Equivalent Height (h^{equ})

The core of the approach for determining h^{equ} is that the magnetic field, at a reasonable distance, produced by the 6-wire bundle should be close to that by an equivalent single-wire. For any short segment of the 6-wire bundle, the current distribution is constant as long as the length is small compared to the shortest wavelength. Since TEM or quasi-TEM mode is dominant, Ampere's Law can be used to calculate the magnetic field produced by each wire. Then, the total H-field produced by the six wires above the ground plane can be obtained using the superposition theory and image theory. Since the current distributions are known for any segment of the bundle, a optimal h^{equ} is selected so that the equivalent H-field produced by the equivalent single-wire approaches the real H-field by the six-wire as closely as possible, as shown in Figure 7. Since h^{equ} is a function of frequency or time, and a function of the position variance along the bundle, the average value of h^{equ} should be selected for the single-wire common-mode circuit model if the value of h^{equ} fluctuates within a small range. Otherwise multiple segments of a single-wire common-mode circuit model, which has different h^{equ}, will be considered. In this homogeneous Case 3, the value of h^{equ} is approximately 14.6-mm, and it is lower than Wire 1, higher than Wire 2 in Figure 6(b).
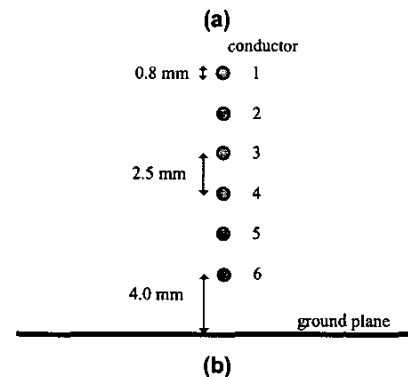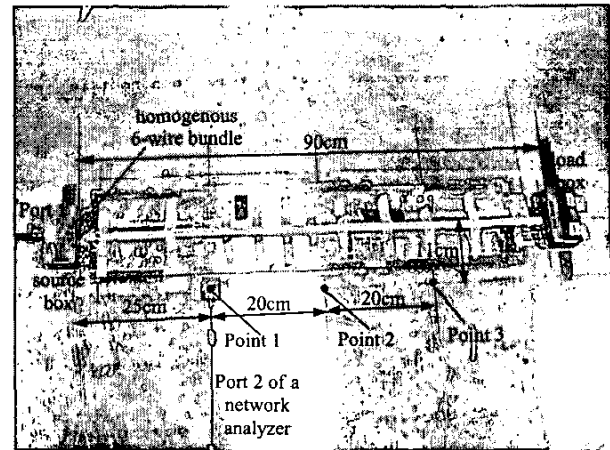

(a)

(b)

Figure 6. Measurement setup of a uniform 6-wire bundle in Case 3: (a) the bundle connecting to the source and load box above the ground plane; (b) 2D cross section of the wire bundle.
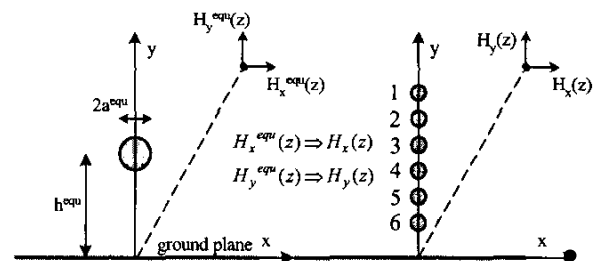
Figure 7. Illustration of the approach for determining h^{equ}.

Equivalent Radius (a^{equ})

The subject of electromagnetic equivalences as applied to wire cage antenna models has been previously studied in [11], [5]. An equivalence was developed for a cage antenna consisting of identical conductors of finite length placed around a circle. The equivalence provided a single conductor of the same length, so that the total axial current distribution is the same in both cases [11]. The key to accurate exploitation of the equivalent radius concept is the proper location of the virtual surface relative to the original cable bundle [5]. In general, a^{equ} is a function of frequency and 2D cross-section of the cable bundle. However, if the

cross-section diameter of the bundle is electrically small, a frequency-independent a^{equ} for the unloaded, uniform, wire-cage bundle is obtained [11], [5],

$$a^{equ} = \sqrt[N]{aD_{12}D_{13}D_{14}\cdots D_{1m}\cdots D_{1N}} , \qquad (2)$$

where a is the radius of each wire, D_{1m} is the distance between Wire m and Wire 1(reference conductor). In Case 3, the 6-wire bundle is not placed around a circle, however, (2) can still provide a good engineering estimate. If the reference conductor is selected as Wire 3, i.e., the feeding wire, then a^{equ} is approximately equal to 2.8-mm, much larger compared to the real radius of each wire, 0.8-mm.

Single-Wire Common-Mode Circuit Model 1

Since h^{equ} and a^{equ} of an equivalent single-wire above the ground plane are determined, the per-unit-length L^{equ} and C^{equ} of the transmission-line can be characterized [8]. Thus, a transmission-line equation can be written as

$$\frac{\partial}{\partial z}V_{cm}(z,t) = -L^{equ}\frac{\partial}{\partial t}I_{cm}(z,t) , \qquad (3)$$

$$\frac{\partial}{\partial z}I_{cm}(z,t) = -C^{equ}\frac{\partial}{\partial t}V_{cm}(z,t) . \qquad (4)$$

To guarantee (3) and (4) to be correct, the common-mode voltage, $V_{cm}(z,t)$ should be defined as

$$V_{cm}(z) = K_{v1}V_1(z) + K_{v2}V_2(z) + K_{v3}V_3(z) + \\ K_{v4}V_4(z) + K_{v5}V_5(z) + K_{v6}V_6(z) = \overline{K}_v\overline{V}(z) , \qquad (5)$$

and two identities must be satisfied,

$$\overline{K}_v\overline{\overline{L}} = L^{equ}\begin{bmatrix} 1 & 1 & 1 & 1 & 1 & 1 \end{bmatrix}, \qquad (6)$$

$$\begin{bmatrix} 1 & 1 & 1 & 1 & 1 & 1 \end{bmatrix}\overline{\overline{C}} = C^{equ}\overline{K}_v , \qquad (7)$$

where K_{vi} (i = 1, ...6) is the voltage coefficient, $V_i(z)$ is the real voltage between the ith wire and the ground plane, $\overline{\overline{L}}$ is the 6×6 per-unit-length inductance matrix for the 6-wire bundle, and $\overline{\overline{C}}$ is the 6×6 per-unit-length capacitance matrix. From (6) or (7), the voltage coefficient vector $\overline{K}_v$ is determined, and the common-mode voltage $V_{cm}(z)$ in Case 3 is defined as

$$V_{cm}(z) = 0.25\,V_1(z) + 0.15\,V_2(z) + 0.14\,V_3(z) + \\ 0.16\,V_4(z) + 0.23\,V_5(z) + 0.52\,V_6(z) . \qquad (8)$$

At both ends of the 6-wire bundle, two boundary conditions, i.e., KVLs, should be satisfied. The similarity transformations can be used to decouple the voltages and currents at the ends. Consequently the diagonal source and load matrices are transformed into two dense matrices. There is a diagonal element in the transformed source matrix corresponding to the defined common-mode, and it is defined as the common-mode source impedance. It equals to

$$Z_{cm,src} = K^2_{v1}Z_{s1} + K_{v2}^2Z_{s2} + K_{v3}^2Z_{s3} + \\ K_{v4}^2Z_{s4} + K^2_{v5}Z_{s5} + K^2_{v6}Z_{s6} \approx 4M\Omega . \qquad (9)$$

Similarly the common-mode load impedance is defined as

$$Z_{cm,load} = K^2_{v1}Z_{l1} + K_{v2}^2Z_{l2} + K_{v3}^2Z_{l3} + \\ K_{v4}^2Z_{l4} + K^2_{v5}Z_{l5} + K^2_{v6}Z_{l6} \approx 20\Omega . \qquad (10)$$

Therefore, a voltage source at the source end, which includes both the original feeding source and the possible mode-conversion effects, is obtained from the source boundary condition, i.e.,

$$V_{cm,src} = V_{cm}(z = 0) + Z_{cm,src}I_{cm}(z = 0) , \qquad (11)$$

At the load end, there is no feeding source, however, the mode-conversion results in a voltage source, i.e.,

$$V_{cm,load} = V_{cm}(z = 90cm) - Z_{cm,load}I_{cm}(z = 90cm) . \qquad (12)$$

The single-wire common-mode circuit model is illustrated in Figure 8(a). Herein the uncertainties of h^{equ} and a^{equ} result in the non-unique definitions of the common-mode voltage and common-mode impedance.

Single-Wire Common-Mode Circuit Model 2

To avoid the ambiguous definitions of common-mode voltage and common-mode impedance, an alternative time-domain single-wire common-mode circuit model is proposed in Figure 8(b). Based on the known h^{equ} and a^{equ}, the characteristic impedance of the equivalent transmission line is characterized as Z_0. Herein the source termination is selected as Z_0, and it absorbs the backward-travelling common-mode current wave reaching the source end. The load termination is also selected as Z_0, and it absorbs the forward-travelling common-mode current wave reaching the load end. The voltage source at the source end $V_{cm,src}(t)$ generates the forward-traveling waves at the time interval $[2mT, (2m+1)T]$, where $m = 0, 1, 2, \dots, T$ is the time delay from one end to the other end. On the other end, the voltage source at the load end $V_{cm,load}(t)$ generates the backward-travelling waves at the time interval $[(2m+1)T, (2m+2)T]$. All these information is derived from a time-domain MTL analysis. This common-mode circuit model can be directly incorporated into FDTD modelling for predicting electric fields. Actually the exact value of a^{equ} is not mandatory in this model since a corresponding Z_0 can always be found based on the approximate a^{equ}.

The predicted electric fields by the two different single-wire common-mode circuit models agree well with the measured in Figure 9. The peaks correspond to the half-wavelength resonances of the 90-cm long bundle. Three dips near the three peaks can be seen on the measured electric field result. These may be caused by the measurement artifacts, e.g., the non-uniform spacing between the nearby wires. High-order connector effects, which are not considered in the MTL modeling, may result in the discrepancy between the measured and predicted electric field results at higher frequencies.
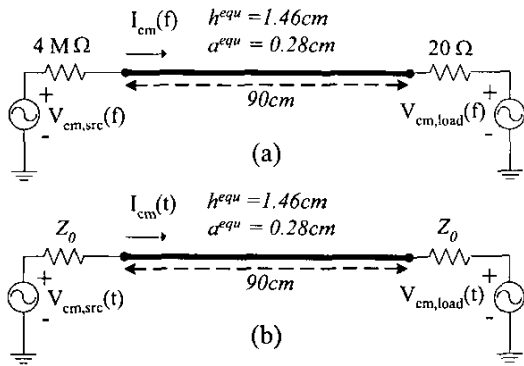
$I_{cm}(f)$ $h^{equ} = 1.46cm$
4 MΩ $a^{equ} = 0.28cm$ 20 Ω

$V_{cm,src}(f)$ 90cm $V_{cm,load}(f)$

(a)

$I_{cm}(t)$ $h^{equ} = 1.46cm$
Z_0 $a^{equ} = 0.28cm$ Z_0

$V_{cm,src}(t)$ 90cm $V_{cm,load}(t)$

(b)

Figure 8. (a) Single-wire common-mode circuit model 1; (b) single-wire common-mode circuit model 2.
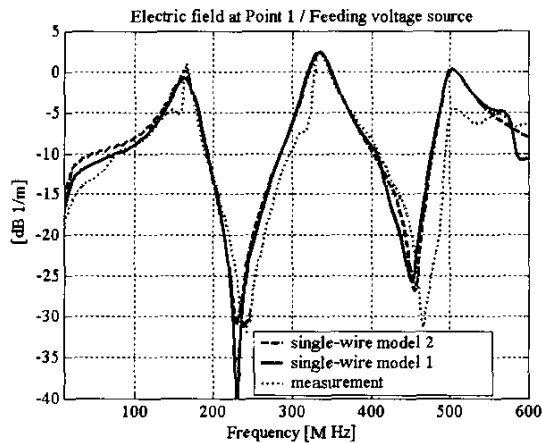

Figure 9. Electric fields at Point 1 in Case 3.

CONCLUSIONS AND FUTURE WORK

This paper proposes a multi-step procedure for predicting vehicle-level EMI. In the first step, the currents on the cable bundles above the vehicle chassis are calculated using MTL modelling. In the second step, a single-wire common-mode circuit model is extracted and incorporated into a FDTD modelling for anticipating vehicle-level EMI. Although the definition of common-mode voltage and common-mode impedance are ambiguous, reasonable approaches for extracting the common-mode circuit are investigated. It is noticed that mode-dispersion caused by the inhomogeneous environment has influences on the extraction of the common-mode circuit model. However, the lump mode-conversion at the ends may alleviate or exacerbate the mode-dispersion phenomenon.

In the homogenous case, reasonable approaches are used to determine the equivalent height and radius of the common-mode circuit model. Although the definitions of the common-mode voltage and common-mode impedance are not unique, they are still used to construct the single-wire model 1. In addition, to avoid using the two ambiguous terms, the time-domain single-wire model 2 is also proposed for predicting EMI. Both common-mode circuit models can provide good electric field estimates. In the

inhomogeneous case, N single-wire sub-common-mode circuits corresponding to the N different mode-velocities must be extracted, and the total radiation can be considered as the superposition of the radiation from the N sub-common-mode circuit models. This approach is possible, yet time-consuming.

In the future, a more appropriate multi-wire model in FDTD will be proposed for conveniently dealing with inhomogeneous case, and typical cases for automotive harness, e.g., slots in the chassis, and branches of cable bundles.

REFERENCES

[1] A. Englmaier, B. Scholl, R. Weigel, and P. Fusser, "EMC modeling strategy for automotive applications", from SimLab Software, Munich, Germany.

[2] M. Troescher, "Analysis of industrial cable harness", SimLab Software, Munich, Germany.

[3] L. Paletta, J-P. Parmantier, F. Issa, P. Dumas, and J-C. Alliot, "Susceptibility analysis of wiring in a complex system combing a 3-D solver and a transmission-line network simulation", *IEEE Transaction on Electromagnetic Compatibility*, vol.44, no.2, May 2002, pp. 309-317.

[4] J. P. Berenger, "A multiwire formalism for the FDTD method", *IEEE Transaction on Electromagnetic Compatibility*, vol. 42, no. 3, August 2002, pp. 257-264.

[5] K. R. Umashankar, A. Taflove, and B. Beker, "Calculation and experimental validation of Induced currents on coupled wires in a arbitrary shaped cavity", *IEEE Transactions on Antenna and Propagation*, vol. AP-35, no. 11, November 1987, pp. 1248-1257.

[6] A. J. Wlodarczyk, V. Trenkic, R. A. Scaramuzza and C. Christopoulos, "A fully integrated multiconductor model for TLM", *IEEE Transaction on Microwave Theory and Techniques*, vol. 46, no. 12, December 1998, pp.2431-2437.

[7] F. M. Tesche, M. Ianoz, and T. Karlsson, *EMC: Analysis Methods and Computational Models*, New York: Wiley, 1997.

[8] C. R. Paul, *Analysis of Multiconductor Transmission Lines*, New York, NY: John Wiley & Sons, Inc., 1994.

[9] A. Taflove, Computational *Electrodynamics: The Finite-Difference Time-Domain Method*, Norwood, MA: Artech House, Inc., 1995.

[10] Geing Liu, Yimin Ding, Chingchi Chen, Richard W. Kautz, James L. Drewniak, David J. Pommerenke, and Marina Y. Koledintseva, "A dual-current-probe method for characterizing common-mode loop impedance", accepted by *2003 IEEE IMTC*, Vail, CO, U.S.A, May 2003.

[11] R. W. P. King, *The Theory of Linear Antennas*, Cambridge, MA: Harvard Univ. Press, 1956

424